Int. J Solids Structures, 1966, Vol 2, pp 467 to 491. Pergamon Press Ltd. Printed in Great Britain

KOROTKOFF SOUNDS AT DIASTOLE—A PHENOMENON OF DYNAMIC INSTABILITY OF FLUID-FILLED SHELLS*

MAX ANLIKER† and K. R. RAMAN‡

Abstract—A theoretical analysis of the phenomenon of Korotkoff sounds at diastole is presented together with experimental results. The formulation of the mathematical analysis is based on facts derived from fundamental experiments with a laboratory model which simulates the brachial artery and the sphygmomanometer and which exhibits Korotkoff sounds under controlled conditions. The Korotkoff sounds at diastole are interpreted as a phenomenon of dynamic instability (oscillations with increasing amplitude), the instability being induced by the application of a pressure cuff. The results of the analysis verify experimental observations regarding the effects of the cuff length, wall thickness and elasticity of the vessel on the diastolic pressure. They also yield good approximations for the difference between the auscultatory diastolic pressure and the true minimum of the pressure in the simulated artery as well as in the human brachial. The results indicate that the auscultatory reading is always higher than the true minimum of the intraluminal pressure by an amount that depends on the physical and geometric properties of the vessel. Besides this, the theoretical analysis predicts that the Korotkoff sounds near the diastolic pressure have predominantly low frequency components and that with *in*creasing cuff pressure the sounds not only become more intense but also begin to include components with a higher pitch.

NOTATION

a	radius of the middle surface at equilibrium configuration (cm)
c^2	nondimensional parameter, $\frac{h^2}{12a^2}$
C_f	the speed of sound of the fluid (cm/sec)
C_G	group velocity (cm/sec)
C_w	phase velocity of moving disturbance (cm/sec)
f	frequency of disturbance (cps)
h	thickness of vessel wall (cm)
k	wave parameter, $\frac{2\pi}{\lambda}$
m_f	apparent mass of the fluid per unit area (g/cm^2)
p_d	auscultatory diastolic pressure (dyn/cm^2 or mm Hg)
p_e	external (or cuff) pressure (dyn/cm^2)
p_i	perturbed intra-arterial pressure (dyn/cm^2)
p_{io}	unperturbed quasi-static intra-arterial pressure (dyn/cm^2)
Δp	transmural pressure $p_{io}-p_e$ (dyn/cm^2)
Δp_c	critical value of Δp at which system becomes unstable
q_1	nondimensional axial stress resultant, $\frac{T_{10}(1-\nu^2)}{Eh}$
q_2	nondimensional circumferential stress resultant, $\frac{a\Delta p(1-\nu^2)}{Eh}$
r	radial coordinate (cm)
s	number of waves in the circumferential direction

* Supported in part by the Ames Research Center of the NASA through contract NAS 2-1137 awarded to Vidya, a Division of Itek Corporation, and by the National Academy of Sciences—National Research Council.

† Department of Aeronautics and Astronautics, Stanford University; currently with Division of Environmental Biology, Ames Research Center of the NASA.

‡ Vidya, A Division of Itek Corporation.

t	time (sec)
u, v, w	small displacement of a general point of the middle surface from equilibrium in the axial, circumferential, and radial directions, respectively
$\mathbf{v}$	perturbation velocity of a fluid particle
x	axial coordinate
$A_{sk}, B_{sk}, C_{sk}, D_{sk}$	coefficients defined in equation (16)
E	Young's modulus of vessel wall (dyn/cm^2)
I_s	modified Bessel function of the first kind of order s
L	length of the pressure cuff (cm)
L_{ij}	linear partial differential operators
R_1, R_2	principal radii of curvature of the middle surface (cm)
R_1°, R_2°	values of R_1 and R_2 for unperturbed equilibrium configuration (cm)
T_1, T_2	resultant tensions in the axial and circumferential directions (dyn/cm)
T_1°, T_2°	values of T_1 and T_2 for unperturbed equilibrium
$T_{1\,0}$	initial axial tension (tonus) of the vessel (dyn/cm)
α	nondimensional axial coordinate, $\frac{x}{a}$
β	circumferential coordinate
γ	wave amplitude
ε	phase angle
ζ	$\left(k^2a^2-\frac{\omega^2a^2}{C_f^2}\right)^{\frac{1}{2}}$
λ	wavelength of disturbance (cm)
μ_f	parameter associated with the inertia of the fluid, $\frac{1-\nu^2}{Eh}a^2m_f$ (sec^2)
μ_w	parameter associated with the inertia of the vessel wall, $\frac{1-\nu^2}{Eh}a^2\rho_w h$ (sec^2)
ν	Poisson's ratio
ρ_f	density of the fluid (g/cm^3)
ρ_w	density of the vessel (g/cm^3)
σ	circular frequency (rad/sec)
τ_0	duration of the unstable phase of the cardiac cycle (sec)
τ_1	duration of the disturbance to travel through the cuff (sec)
ϕ, ϕ_{sk}, Φ	velocity potential of perturbed fluid motion (cm^2/sec)
χ	$\rho_f a\frac{I_s(\zeta)}{\zeta I_s'(\zeta)}$ a complex quantity
ω	circular frequency of perturbation
∇^2	Laplacian operator

1. INTRODUCTION

AMONG the many diagnostic parameters used in clinical medicine, the arterial blood pressure is of particular significance. It is not only instrumental in the diagnosis of many diseases but also a measure of cardiovascular performance. Even though the blood pressure varies greatly within the circulatory system, the usual meaning of the term "blood pressure" is the pressure in the brachial artery in the upper arm. There are several ways in which the pressure in blood vessels can be determined. A state-of-the-art summary, with a brief historical review and an extensive reference list pertaining to this topic, is given in a NASA publication by Smith and Bickley [1] which is oriented primarily toward nonmedical scientists and engineers.

The methods of measuring blood pressure can be divided into two major categories: *direct* and *indirect* methods. The direct methods make use of pressure sensing devices which are inserted into the blood vessel of interest. The indirect techniques rely on a reaction to the blood pressure that can be measured outside that part of the body in which the vessel of interest is located. While the direct techniques offer reliable and accurate values for the blood pressure and can be applied to most parts of the circulatory

system, including a heart cavity, they are not widely used since they require the penetration of arteries or veins with foreign objects and thus involve the risk of infection.

The variation of the pressure in the brachial or other large arteries with time is graphically illustrated in Fig. 1. The maximum or *systolic pressure* occurs during the

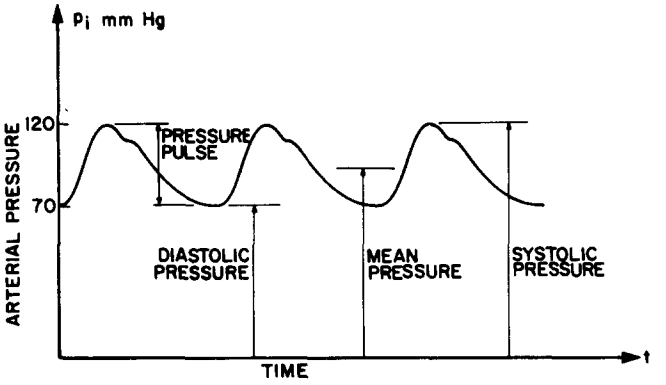

FIG. 1. Pressure variation in brachial or other large artery during cardiac cycle.

contraction of the heart while the minimum or *diastolic pressure* is the residual pressure at the instant of opening of the aortic valve. According to the medical literature, a healthy young adult has normally a systolic pressure of approximately 120 mm Hg and a diastolic pressure of 70 mm Hg. (In stating these figures it should be emphasized that the blood pressure is controlled by numerous biological factors as well as the emotional state of the person.) The difference between systolic and diastolic pressure is the *pulse pressure.* The arithmetic mean of systolic and diastolic pressure is usually referred to as the *mean pressure.* The arithmetic mean is somewhat higher than the integrated mean pressure, since the period of contraction (systole) is shorter than that of expansion (diastole).

Among the indirect methods of measuring the blood pressure, the so-called *auscultatory* technique, which makes use of the phenomenon of Korotkoff sounds, is most widely used. This technique was introduced in the early 1900's and is essentially a modification of a method devised by Riva-Rocci in 1896. As an indirect way of determining the systolic pressure, Riva-Rocci suggested the use of a pneumatic cuff to measure the compression pressure required to obliterate the pulse. The pneumatic cuff used for this purpose is referred to as a cuff sphygmomanometer. A modern sphygmomanometer consists of a compression bag with an adjustable cuff, a manometer to measure the applied pressure, a hand pump and a controllable exhaust that allows a gradual reduction of the pressure. Using such a sphygmomanometer, the auscultatory technique allows an approximate determination of both the systolic and diastolic pressures in certain arteries. In the usual application of the auscultatory technique [2], the cuff is wrapped around the upper arm and secured. To minimize effects of gravity, the person is placed in such a position that his heart is at the same level as the cuff. A stethoscope is placed over the brachial artery at the elbow and the cuff is rapidly inflated to a pressure level of approximately 30 mm Hg above the point at which the artery remains fully occluded during the entire cardiac cycle, that is, 30 mm Hg above the pressure at which the pulse is fully obliterated. The cuff pressure is then gradually reduced at a rate of approximately 3–5 mm Hg/sec. As

soon as the cuff pressure drops to a certain critical limit, one begins to hear with each beat a characteristic kind of tapping sounds, which are called Korotkoff sounds. As the cuff pressure is reduced further, these sounds become louder, then dull and muffled, and finally disappear at a certain lower critical limit of the cuff pressure. The cuff pressure at which the sounds are first heard (upper critical pressure) is interpreted as an approximation of the systolic or maximum pressure, while the cuff pressure at which sounds disappear (lower critical pressure) is interpreted as an approximation of the diastolic or minimum pressure in the artery.

By comparing the readings for diastolic and systolic pressures obtained with the aid of the auscultatory technique with corresponding values determined by direct methods, it was observed that under normal conditions and for a healthy person the results may differ by as much as 8 mm Hg. For certain patients, however, it is possible that the relative differences may exceed 25 per cent [3].

A review of the medical literature indicates that the basic mechanism by which the Korotkoff sounds are produced has so far not been fully understood. There are, though, various hypotheses that have been advanced to explain the cause of sound production [4–12], but none of them has been substantiated by a theoretical analysis, and in most cases no conclusive experimental evidence was produced to corroborate the suggested mechanism. A better understanding of Korotkoff sound production is not only of general scientific interest but is also highly desirable in view of the strong reliance of clinical and space medicine on the auscultatory technique.

It is generally accepted that the Korotkoff sounds are distinct and separate from heart sounds and murmurs. Some authors studied only the murmurs accompanying the Korotkoff sounds. After investigating the cardiovascular sounds McKusick [13] postulated that the high-pitch murmurs following the Korotkoff sounds are due to eddy and turbulence.

Scattered through the literature we find some qualitative data relating the cuff pressure and the frequency spectrum of the Korotkoff sounds [14–17]. Although these data are fragmentary they indicate that the spectrum extends from approximately 20 to 500 cps. The possibility that the frequency spectrum and its variation with cuff pressure may reveal pertinent information on the circulation (for example, signs of impending cardiovascular collapse during surgery) can be considered as an additional incentive for further research on the mechanism of Korotkoff sound generation.

2. LABORATORY EXPERIMENTS PERTAINING TO THE PRODUCTION OF KOROTKOFF SOUNDS ON A SIMULATED ARTERY

Some experimental studies with simulated arteries were recently made by Sacks *et al.* [18] in order to investigate the relationship between the indirectly determined blood pressure and the actual arterial pressure. Using a properly scaled pressure cuff, they have demonstrated that pulsatile flow through rubber tubes exhibits the entire spectrum of Korotkoff sounds and thus permits the study of the auscultatory method under controlled conditions. They have shown that the effects of viscosity are relatively small since Korotkoff sounds could be produced with test fluids having a kinematic viscosity between 1 and 30 cm^2/sec. (Blood has a kinematic viscosity of approximately 5 cm^2/sec, water 1 cm^2/sec.) Also, it appears that the compressibility of the fluid is not essential to the generation of the sounds since they were observed with both fresh steer blood and pure

water. Moreover, effects of anisotropy and viscoelasticity of the vessel material seem not to play a significant role, considering that the rubber tubes which exhibited Korotkoff sounds showed no noticeable anisotropy and hysteresis under the prevailing conditions given by the initial stresses (initial axial strain 20 per cent to simulate the tonus), the blood flow and the surrounding medium. However, it was demonstrated that the elasticity of the vessel wall has a marked influence on the auscultatory readings.

The inherent complexity of circulatory problems and the numerous parameters associated with them renders a realistic theoretical study rather formidable. A critical review of various attempts in the mathematical analysis of blood flow was recently published by Fox and Saibel [19]. To establish a minimal basis for a simple mathematical formulation of the dynamic behavior of the brachial artery and its laboratory model, the authors conducted a number of additional fundamental experiments [20]. For this purpose the facility described in [18] and illustrated schematically in Fig. 2 was modified.

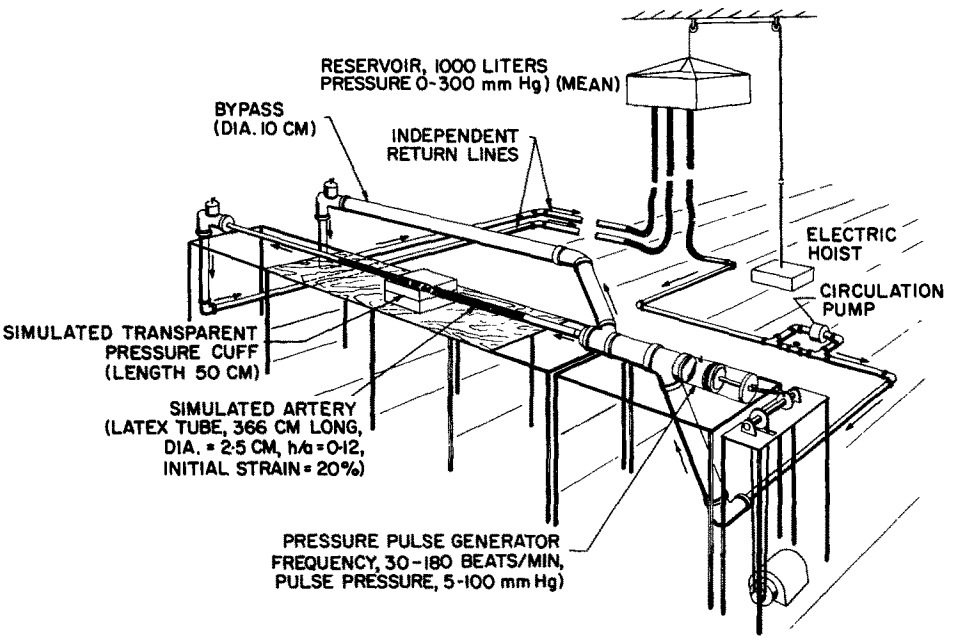

FIG. 2. Schematic sketch of experimental apparatus.

By using a transparent pressure chamber and a translucent latex tube as the simulated artery it was possible to observe some of the characteristic behavior of the vessel wall and the fluid during the production of Korotkoff sounds. Visualization of the dynamic behavior of the system was attained by adding food coloring to the test fluid. Movies and continuous recordings of pressures and sounds were made. Representative samples of the data are given in Figs. 3 and 4.

Some of the results of the experiments conducted with the modified laboratory model call for a revision of the widely accepted notions regarding the dynamic behavior of the artery and the blood flow during Korotkoff sound generation. For example, from movies and direct visual observations the following conclusions may be drawn:

(1) There is an established fluid flow prior to the actual onset of the Korotkoff sounds, i.e. at cuff pressures slightly above the systolic.
(2) The simulated artery is not fully occluded during any phase of Korotkoff sound production.
(3) At diastolic cuff pressures the simulated artery undergoes only small deformations and thus essentially retains its circular cylindrical shape during the entire cardiac cycle. (This is, of course, not surprising since for near diastolic cuff pressures the intraluminal pressure p_i exceeds the external pressure p_e during most of the cardiac cycle and thus the time during which $p_i < p_e$ is too short to allow the prevailing forces to induce the collapse of the vessel.)
(4) Flow visualization with the aid of dye tracers does not reveal any turbulent bursts or vortex shedding.

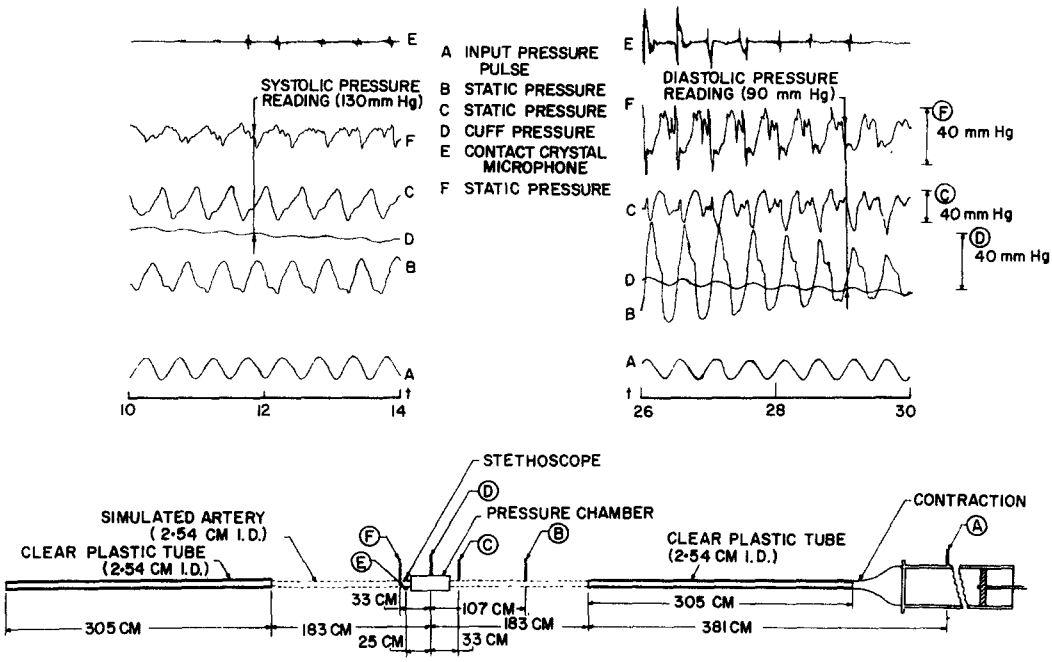

FIG. 4. Oscillograph record of static pressures at various axial locations during cuff decompression.

Besides this we find from pressure recordings that the group velocity (pulse velocity) increases rapidly with decreasing cuff pressure. For example, with the simulated artery described in [20] the group velocity increases by approximately a factor of two between systolic and diastolic pressures. The results of pulse velocity measurements for the entire range of cuff pressures, obtained by monitoring the static pressures at two axial positions, are given in Fig. 5.

In a recent publication on the genesis of Korotkoff sounds Chungcharoen [11] implies that the flexibility of the vessel and its surrounding have no influence on the generation of the sounds. Evidence contradicting this implication was established by the following experiments:

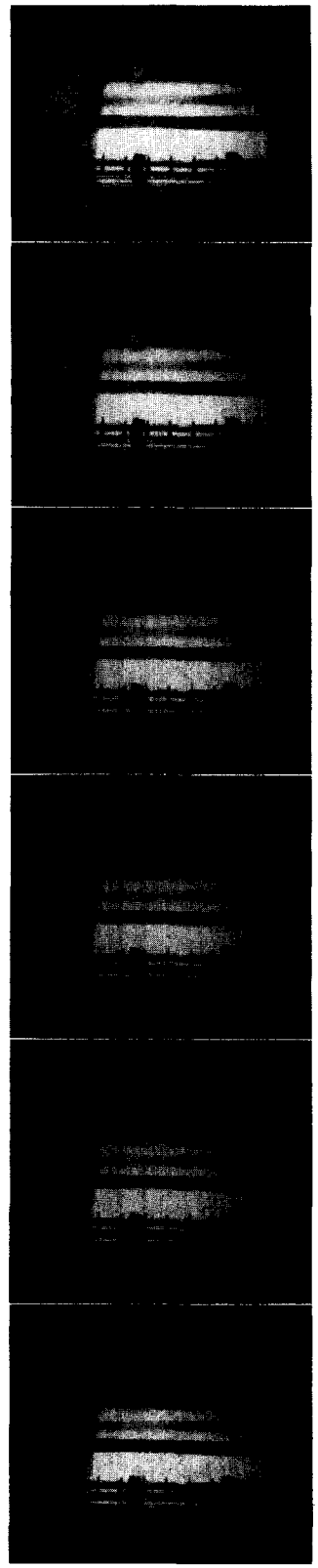

FIG. 3. Motion pictures showing pulse wave propagation (right to left) during partial occlusion of artery.

[*facing page* 472

(a) The elastic diaphragms of the simulated pressure cuff that sandwich the rubber tube were replaced by rigid wooden blocks. A gradual reduction of the pressure on the simulated artery induced by these blocks from a pressure level corresponding to complete occlusion did not lead to audible Korotkoff sounds or other audible sounds at any time.
(b) If a pair of moderately flexible Neoprene sheets (0·15 cm thick) were used as diaphragms instead of the rigid wooden blocks, again no sounds could be heard.
(c) With highly flexible Dental Dam sheets (0·02 cm thick) as diaphragms, Korotkoff sounds of high intensity were produced, as in [18].
(d) Korotkoff sounds could also be heard when each diaphragm consisted of two Dental Dam sheets with foam rubber sandwiched in between to simulate the soft tissue surrounding the brachial artery. However, the simulation of the soft tissue led to higher systolic and diastolic pressures and caused the Korotkoff sounds to be muffled compared with those generated without the foam rubber.

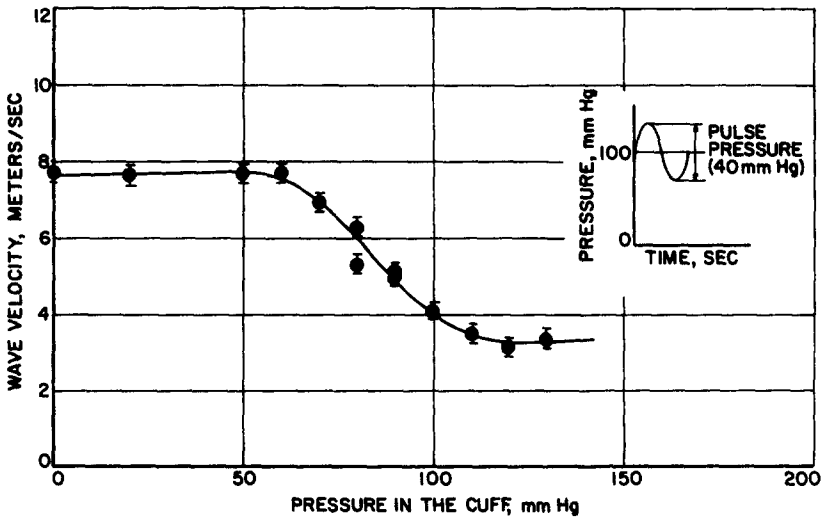

FIG. 5. Pulse wave velocity in simulated artery as a function of cuff pressure. The velocities were obtained by monitoring the static pressures at two axial positions.

3. A NEW HYPOTHESIS FOR THE GENERATION OF KOROTKOFF SOUNDS

Like any other sound perceived by a human ear, the Korotkoff sounds heard with the aid of the stethoscope are aggregates of vibrations whose frequencies and intensity place them within the audibility range. It is conceivable that the Korotkoff sounds are due to disturbances in the flow that are induced locally, that is, in the segment of the brachial artery which is compressed by the cuff. However, it is also possible that they are a part of the noise associated with pulsatile flow through the circulatory system that is selectively amplified to a level above the audibility threshold in the compressed section of the brachial. It is well known that pulsating flow through the complex system of blood vessels generates a multitude of wave motions; the associated vibrations are not audible because their

amplitudes and in many cases their frequencies are far below the audibility threshold [21]. Irrespective of the origin of the disturbances leading to Korotkoff sounds, it will be shown that the application of a pressure cuff can change the system locally from one that is dynamically stable to one that is intermittently unstable and thus capable of mechanically amplifying certain low intensity vibrations (disturbances) to such an extent that they become audible. The dynamic stability of the compressed brachial artery is examined by studying its dynamic response to small disturbances. The response in this case is the displacement of a general point of the middle surface of the artery from its equilibrium position and its velocity.

In a preliminary analysis, only "stationary" perturbations are considered, even though in reality it is the moving disturbance that is observed as a sound. This means that in a first approximation the inertia effects associated with the propagation are disregarded and the system interpreted as unstable for moving disturbances whenever it is found unstable for "stationary" perturbations. In view of the large axial strains associated with the initial tension in the wall, the equilibrium configuration of the vessel for a given pressure difference Δp between the inside and the surrounding medium (transmural pressure) may have to be determined by a nonlinear theory. However, in determining the response to small perturbations of the equilibrium configuration it is assumed that the system is linear. Thus the classical methods of linear elastic stability analysis [22–24] can be applied and the stability analysis be reduced to the study of free small vibrations of the system under the prevailing conditions given by the tonus Δp and the surrounding medium.

Considering that the pulse frequency is of the order 1 cps and the audible frequency range of the Korotkoff sounds approximately 20–500 cps, the variation of the intraluminal pressure p_{io} during the period of any one of the sound components can be neglected. Hence, for the purpose of investigating the amplification of these sound components the intra-arterial pressure can be considered as quasi-static. If the external pressure p_e exerted by the cuff on the brachial artery is gradually increased from zero (this is contrary to the clinical procedure but more convenient for theoretical considerations), one expects the system to become unstable and behave like a mechanical amplifier as soon as the pressure difference $\Delta p = p_{io} - p_e$ between the quasi-static internal and external pressures approaches a critical limit value $(\Delta p)_{crit}$. The duration τ_0 and the degree of instability is, of course, dependent on Δp as graphically illustrated in Fig. 6 in which the time-dependence of the arterial pressure is given by a sine wave and the cuff pressure is restricted to levels corresponding to the diastolic phase. For small cuff pressures p_e the system is stable and no amplification takes place, as indicated in case (a) of Fig. 6. However, for sufficiently high cuff pressures Δp exceeds intermittently the critical limit $(\Delta p)_{crit}$, as assumed in cases (b), (c) and (d), and during the corresponding time interval τ_0 certain disturbances grow exponentially as they propagate through the compressed section of the brachial artery. (Note that $(\Delta p)_{crit}$ is assumed to be negative in this illustration.) When these amplified disturbances leave the unstable segment of the artery or when the pressure cycle reenters the stable phase, dissipative mechanisms which are disregarded in a preliminary stability analysis are responsible for the attenuation of the response. In case (b) of Fig. 6 the cuff pressure is increased to a level at which $p_{io} - p_e$ is below the critical limit for a short time interval τ_0. The duration of the instability at the given cuff pressure and the corresponding amplifications of appropriate disturbances are taken as insufficient to lead to audible sounds. In case (c) the cuff pressure is increased

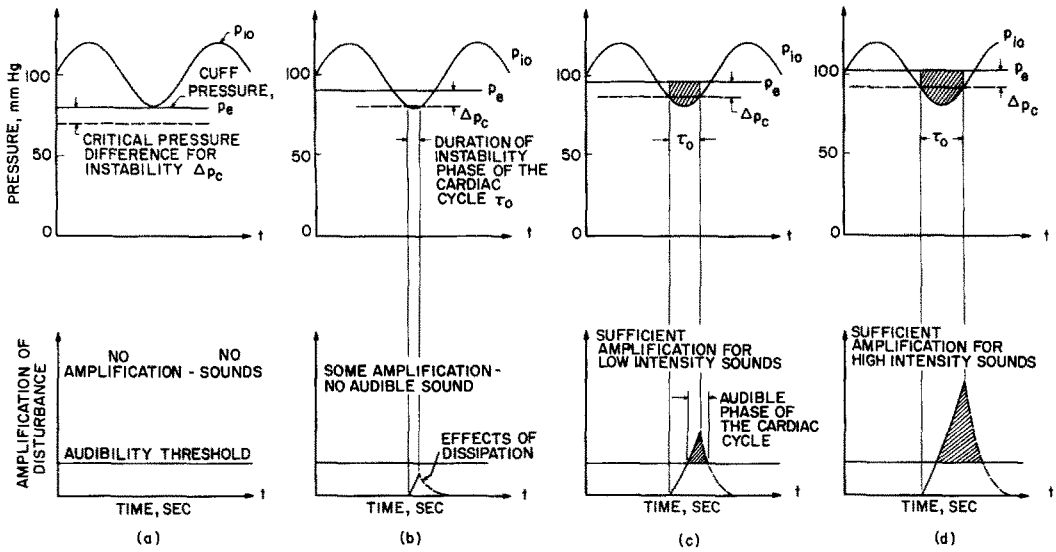

FIG. 6. Unstable phase of the cardiac cycle and its duration at near diastolic cuff pressures. In case (a) the cuff pressure is below the critical value required for instability, hence no sounds are audible. In case (b) the degree and duration of the instability are taken as insufficient to lead to sounds of intensity and frequencies within the audibility range. A further increase of the cuff pressure as shown in cases (c) and (d) results in more intense Korotkoff sounds.

further and the corresponding duration τ_0 of the unstable phase and the amplifications are now sufficient to generate audible sounds. This means that the response of the system to certain disturbances should exceed the audibility threshold. Here the sounds will still be audible as the cardiac cycle reenters the stable phase and persist until attenuated below the audibility threshold. Finally a still further increase in cuff pressure would lead to a corresponding increase in the intensity of the sounds as shown in case (d).

On the basis of our laboratory experiments we may expect that for cuff pressures p_e close to the diastolic pressure p_d the geometric configuration of the compressed brachial artery remains essentially the same throughout the cardiac cycle. However, for higher cuff pressures we must anticipate that the brachial artery assumes a partially collapsed configuration, at least during a part of the pressure cycle. This implies that for cuff pressures p_e above a certain level we have to expect $(\Delta p)_{crit}$ to depend on p_e, and in analyzing the stability of the system we may have to take the variation of the over-all brachial geometry with the intraluminal pressure into consideration, even though this change takes place rather slowly compared with the vibration associated with Korotkoff sounds.

4. THEORETICAL MODEL FOR DIASTOLIC PHASE

For a theoretical analysis we assume the blood vessels to behave like shells made of homogeneous isotropic material and filled with an inviscid incompressible fluid. Considering that the ratio of cuff length to vessel diameter is of the order 20, we shall treat the shell in certain respects as infinitely long. At cuff pressures close to the systolic the simulated artery is partially collapsed and thus assumes an entirely different geometry than at

the diastolic phase. In describing the geometry of the artery in our mathematical analysis we therefore have to make a distinction between these two phases. We shall restrict ourselves to the diastolic phase considerations only, even though we have devised an idealized mathematical model for the systolic case, the exact physical counterpart of which has exhibited Korotkoff sounds in the laboratory.

In view of the fact that the simulated brachial essentially retains its circular cylindrical shape during the diastolic phase of indirect blood pressure measurement, we shall start out from a circular cylindrical shell and determine mathematically the dynamic response of the system at cuff pressures close to diastolic.

5. MATHEMATICAL STABILITY ANALYSIS FOR DIASTOLIC PHASE

For the mathematical analysis of the vibratory motion of the brachial or its laboratory model during the diastolic phase we refer the middle surface of the cylindrical vessel to a set of cylinder coordinates x, β, r as shown in Fig. 7. For a given pressure difference, Δp

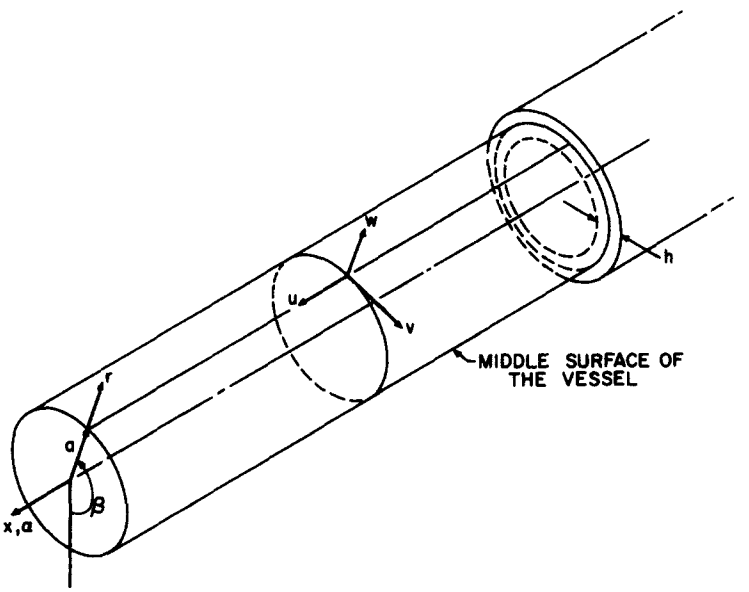

FIG. 7. Coordinate system.

(quasi-static), and prescribed initial axial tension (tonus) the equilibrium configuration of the middle surface (quasi-static) is assumed to be a circular cylinder defined by $r = a$. The displacement of an arbitrary point of the middle surface from its equilibrium position during a small perturbation has the components u, v, w measured in the x, β and r directions respectively. In all our models the material of the vessel wall is considered as having uniform properties. In addition it is always assumed that the flow associated with the disturbance is irrotational and that the effects of a mean flow and of body forces (gravity) can be neglected. This allows us to write the continuity equation in terms of the velocity potential ϕ as

$$\nabla^2\phi = \frac{\partial^2\phi}{\partial x^2}+\frac{1}{r^2}\frac{\partial^2\phi}{\partial\beta^2}+\frac{1}{r}\frac{\partial}{\partial r}\left(r\frac{\partial\phi}{\partial r}\right) = 0 \tag{1}$$

and the linearized Euler equation in the form

$$p_i = \rho_f\frac{\partial\phi}{\partial t}+p_{io} \tag{2}$$

where p_i is the perturbed intra-arterial pressure, ρ_f the density of the fluid, p_{io} the quasi-static internal pressure in the absence of any disturbance ($\phi \equiv 0$). The velocity, $\mathbf{v}$, of the fluid corresponding to the disturbance is related to the velocity potential by

$$\mathbf{v} = -\nabla\phi \tag{3}$$

Adhering consistently to a linearized analysis, we can express the kinematic boundary condition as

$$\frac{\partial w}{\partial t} = -\left(\frac{\partial\phi}{\partial r}\right)_{r=a} \tag{4}$$

At this point it becomes necessary to specify additional characteristic features of the mathematical model for the vessel. For our analysis we shall assume that the vessel behaves first like a membrane and then like a shell, taking into consideration the effects of coupling among the axial, radial and circumferential motions.

5.1 *Simplified Membrane Model*

In a first approximation we neglect the bending rigidity of the vessel wall. Further, we assume that the displacement components u, v, w are completely independent, which allows us to disregard the motion of the vessel wall in the axial and circumferential directions.

As dynamic boundary condition at the middle surface we have

$$p_i - p_e = \frac{T_1}{R_1}+\frac{T_2}{R_2}+\rho_w h\frac{\partial^2 w}{\partial t^2} \tag{5}$$

where R_1 and R_2 are the principal radii of curvature, T_1 and T_2 the corresponding stress resultants and ρ_w the density of the vessel wall. The radii of curvature are taken as positive if the center of curvature lies within the fluid. The force equilibrium in the radial direction as expressed by equation (5) does not account for the fact that the internal pressure p_{io} is acting on a smaller surface area than the external pressure p_e. (This fact is usually ignored since in most investigations the wall thickness is assumed to be very small. A notable exception in this regard was made by Armenakas and Herrmann [25]). In presence of the disturbance w, the equation for the bounding surface can be written as

$$r = a+w(x,\beta,t) \tag{6}$$

With (6) the principal radii of curvature of the wall are in a first approximation given by

$$\frac{1}{R_1} = -\frac{\partial^2 w}{\partial x^2} \tag{7}$$

$$\frac{1}{R_2} = \frac{1}{a}-\frac{1}{a^2}\left(w+\frac{\partial^2 w}{\partial\beta^2}\right) \tag{8}$$

Substituting (7) and (8) into (5) and making use of relation (2), we obtain after linearization

$$p_e = \rho_f\left(\frac{\partial\phi}{\partial t}\right)_{r=a} + T_1\frac{\partial^2 w}{\partial x^2} - \frac{T_2}{a} + \frac{T_2}{a^2}\left(w + \frac{\partial^2 w}{\partial\beta^2}\right) + p_{io} - \rho_w h\frac{\partial^2 w}{\partial t^2} \tag{9}$$

The tension T_1 in the axial direction is the result of an initially applied axial tension T_{10} (the simulated artery was subjected to a strain of 20 per cent), the addition of a transmural pressure $\Delta p = p_{io} - p_e$ and the displacement of the vessel wall from its equilibrium position. Assuming that the ends of the artery are restrained from moving in the axial direction after the application of the initial tension we have

$$T_1 = T_{10} + va\Delta p + v\frac{E}{1-v^2}\frac{h}{a}w \tag{10}$$

where E is Young's modulus and v the Poisson ratio. The radius a of the middle surface of the cylinder defines the equilibrium configuration resulting from the application of the initial axial tension T_{10} and the transmural pressure Δp. The tension in the circumferential direction can be written as

$$T_2 = a\Delta p + \frac{E}{1-v^2}\frac{h}{a}w \tag{11}$$

For $\phi \equiv 0$ (static equilibrium) we have $w \equiv 0$ and

$$\frac{1}{R_1} = \frac{1}{R_1^o} = 0, \qquad \frac{1}{R_2} = \frac{1}{R_2^o} = \frac{1}{a} \tag{12}$$

$$T_1 = T_1^o = T_{10} + va\Delta p \tag{13}$$

$$T_2 = T_2^0 = a\Delta p \tag{14}$$

We know that the pressure pulse induces small fluctuations of the cuff pressure p_e in the diastolic phase. However, since we are primarily interested in the unstable portion of the cardiac cycle, which we expect to be of short duration, we may assume that $p_e = p_{io} - \Delta p$ is independent of the small disturbance. Retaining only linear terms we can therefore express the dynamic boundary condition (9) as

$$\rho_f\left(\frac{\partial\phi}{\partial t}\right)_{r=a} + (T_{10} + va\Delta p)\frac{\partial^2 w}{\partial x^2} - \frac{E}{1-v^2}\frac{h}{a^2}w + \frac{\Delta p}{a}\left(w + \frac{\partial^2 w}{\partial\beta^2}\right) - \rho_w h\frac{\partial^2 w}{\partial t^2} = 0 \tag{15}$$

In addition we assume now that either the boundary conditions at the ends of the compressed portion of the brachial are of an appropriate nature or that we may treat the compressed section as infinitely long. This allows us to give a set of basic solutions of the continuity equation (1) in terms of cylinder coordinates of the form

$$\phi_{sk} = I_s(kr)[A_{sk}\cos(s\beta) + B_{sk}\sin(s\beta)]\ [C_{sk}\cos(kx) + D_{sk}\sin(kx)]\cos(\sigma t - \varepsilon) \tag{16}$$

$$k = \frac{2\pi}{\lambda}, \qquad s = 0, 1, 2, 3, \ldots.$$

where s is the number of waves in the circumferential direction, λ the wave length in the axial direction, ka the corresponding wave number, $I_s(kr)$ the modified Bessel function of order s, and σ the circular frequency of the oscillation. According to (4) the corresponding set of displacements w_{sk} of the bounding surface (artery wall) has the form

$$w_{sk} = -\frac{kaI_s'(ka)}{\sigma a}[A_{sk}\cos(s\beta)+B_{sk}\sin(s\beta)][C_{sk}\cos(kx)+D_{sk}\sin(kx)]\sin(\sigma t-\varepsilon) \tag{17}$$

where

$$I_s'(ka) = \left\{\frac{\mathrm{d}}{\mathrm{d}(kr)}[I_s(kr)]\right\}_{r=a}$$

It should be emphasized that the set of solutions defined by (16) and (17) includes non-axisymmetric disturbances while all investigations on blood flow known to the authors restrict themselves to axially symmetric flow and response, including the recent publications by Mollo-Christensen [26, 27], Lambert [28] and Narasimhan [29]. The circular frequency σ is obtained from the dynamic boundary condition (15) by substituting (16) and (17):

$$\sigma^2 = \frac{1}{\rho_w h+\rho_f\dfrac{aI_s(ka)}{kaI_s'(ka)}}\frac{Eh}{a^2}\left[\frac{1}{1-\nu^2}+\frac{a\Delta p}{Eh}(s^2+\nu k^2a^2-1)+\frac{T_{10}}{Eh}k^2a^2\right] \tag{18}$$

For dynamic stability we must require $\sigma^2 > 0$. We note that instability ($\sigma^2 \leqslant 0$) can occur for $s = 0$ or $s > 0$ depending on the sign of Δp. The amplification of a disturbance during its travel through the unstable segment of the artery is $\exp|\sigma|\tau$ where τ is the smaller value of either the duration τ_0 of the instability or the time τ_1 required for the passage of the disturbance through the cuff ($\tau = \tau_1$ if $\tau_1 < \tau_0$; $\tau = \tau_0$ if $\tau_0 < \tau_1$). Since $|\sigma|$ as well as τ_0 and τ_1 are functions of Δp, we may expect the amplification to depend on Δp. Consistent with the assumption that the intra-arterial pressure can be considered as quasi-static as far as the Korotkoff sound generation is concerned, we introduce an appropriate average for Δp during the unstable phase (see Fig. 8) for an estimate of the amplification.

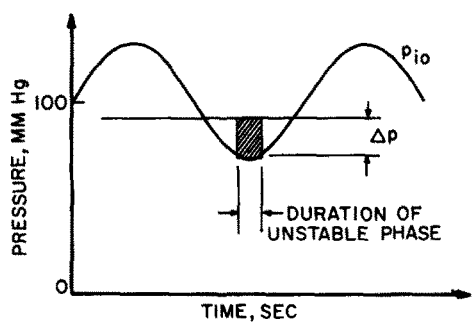

FIG. 8. Average transmural pressure Δp during unstable phase.

Results of membrane analysis

(a) *axisymmetric case* ($s = 0$)

$$\sigma^2 \leqslant 0 \quad \text{if} \quad \begin{cases} \Delta p \geqslant \dfrac{\dfrac{Eh}{1-\nu^2} + T_{10}k^2a^2}{a(1-\nu k^2a^2)}, & \lambda > 2\pi a\sqrt{\nu} \\ \Delta p \leqslant -\dfrac{\dfrac{Eh}{1-\nu^2} + T_{10}k^2a^2}{a(\nu k^2a^2-1)}, & \lambda < 2\pi a\sqrt{\nu} \end{cases} \tag{19}$$

For $\lambda > 2\pi a\sqrt{\nu}$ the transmural pressure Δp required for instability is above the range of interest for Korotkoff sound generation, while for $\lambda < 2\pi a\sqrt{\nu}$ the corresponding Δp is of much greater magnitude than that obtained for $s > 0$.

(b) *nonaxisymmetric case* ($s > 0$)

$$\sigma^2 \leqslant 0 \quad \text{if} \quad \Delta p \leqslant -\frac{\dfrac{Eh}{1-\nu^2} + T_{10}k^2a^2}{a(s^2-1+\nu k^2a^2)} \tag{20}$$

For nonaxisymmetric disturbances and parameters corresponding to the laboratory model described in [20] the amplification factor $\exp|\sigma|\tau$ reaches magnitudes of the order exp 30 (on the basis of a linearized theory, neglecting all dissipation and taking $\tau = 0{\cdot}1$ sec). This means that according to the simplified membrane model only *non*-axisymmetric disturbances lead to Korotkoff sounds. Nonaxisymmetric flow patterns have been observed by Block [30], McDonald and Helps [31] by means of motion pictures which show helical patterns of erythrocyte and dye marker flow. We also note that with increasing s the pressure difference required for instability approaches zero. However, taking into consideration that with increasing s the effects of even a small bending rigidity of the vessel wall can no longer be ignored, we have to impose an upper bound on s, say $s \leqslant 10$, which points out the shortcomings of this simple model. Disregarding this fact, we find that the onset of instability (near the diastolic pressure) depends on the thickness ratio h/a and also on the wave length of the disturbance as illustrated in Fig. 9. On the basis of physical considerations we may restrict the wave length λ in the axial direction to $\lambda \leqslant 2L$, where L is the length of the pressure cuff. As a representative example we obtain for the experimental model described earlier $(\Delta p)_{\text{crit}} \approx -6{\cdot}9$ mm Hg (for $s = 10$ and wave length $\lambda \approx 60$ cm), which means that the auscultatory diastolic pressure is approximately 6·9 mm Hg higher than the minimum intra-arterial pressure of the simulated brachial.

From the graphs in Fig. 9 and from equation (18) we make the following deductions:

(1) The auscultatory diastolic pressure $p_e = p_d$ is always higher than the minimum of the intra-arterial pressure. This is consistent with the observations made with the laboratory model [18].

(2) An increase of the thickness to radius ratio h/a leads to an increase of p_d for a given p_{io} which is also in agreement with the results reported by Sacks *et al.* [18].

(3) An increase of the wave length beyond a certain limit has no noticeable effect on p_d. This implies that there is an optimal length for the pressure cuff beyond which the measurement is unaffected by the cuff length, as pointed out also by Karvonen *et al.* [32].

(4) A limitation to shorter wave lengths (which is equivalent to a reduction in cuff length, since the longest wave length is always twice the cuff length) also results in an increase of p_d.
(5) Likewise, an increase of Young's modulus and/or the initial axial tension T_{10} causes an increase of p_d.
(6) With increasing wall mass $\rho_w h$ the diastolic pressure increases while the intensity of the Korotkoff decreases.

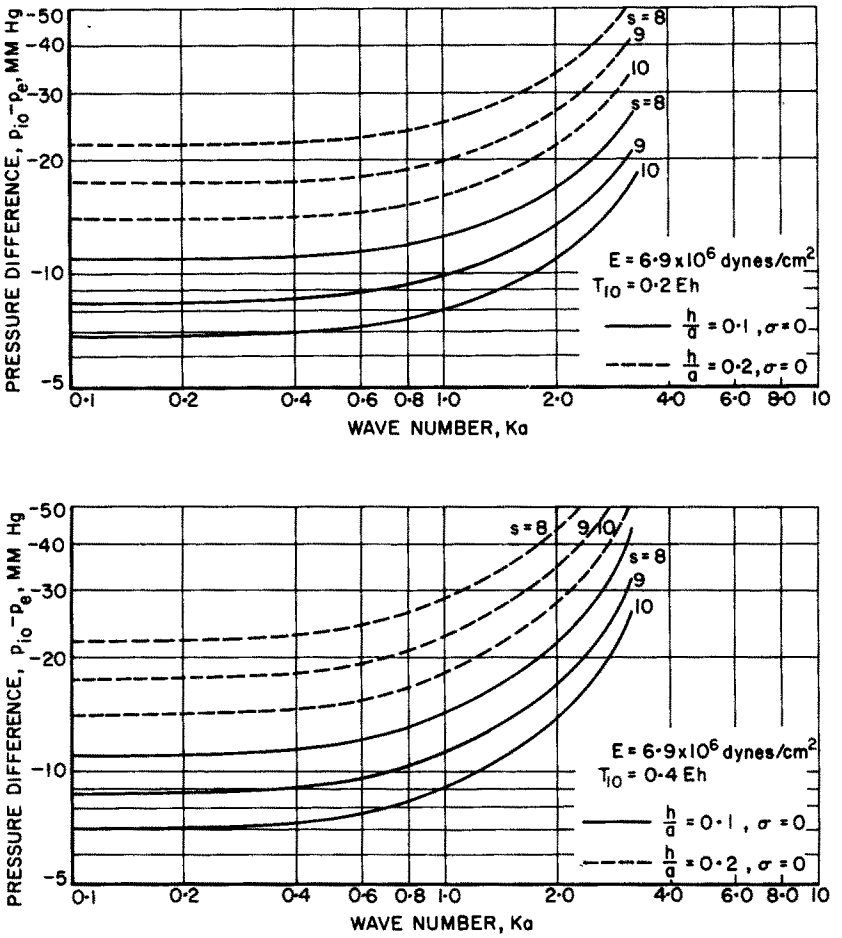

FIG. 9. Stability boundaries for the simplified membrane model.

For the sake of clarity it should be stressed that whenever an increase of p_d for a given p_{io} is effected, the discrepancy between the indirectly measured diastolic pressure and the true minimum of the intra-arterial pressure is increased. Moreover, we should mention that the above facts are verified in the next section (5.2) by a substantially improved theoretical analysis.

5.2 *Shell Model*

For a second approximation we treat the vessel as an isotropic shell with bending rigidity and take the interaction between the axial, circumferential and radial displacement of a general point of the middle surface into consideration. In analyzing the dynamic stability of the system based on this model we make use of the linearized equations for circular cylindrical shells developed by Flügge [33]. We introduce as dimensionless stress resultants in the axial and circumferential directions respectively

$$q_1 = \frac{T_{1\,0}(1-\nu^2)}{Eh} \tag{21}$$

$$q_2 = \frac{a\Delta p}{Eh}(1-\nu^2) \tag{22}$$

Further, we define as nondimensional axial coordinate

$$\alpha = \frac{x}{a} \tag{23}$$

and shall use the abbreviation

$$c^2 = \frac{h^2}{12a^2} \tag{24}$$

$$\nabla^2 = \frac{\partial^2}{\partial\alpha^2} + \frac{\partial^2}{\partial\beta^2} \tag{25}$$

For small displacements from the equilibrium configuration $r = a$ which the shell assumes under uniform axial tension $T_1^0 = T_{1\,0} + \nu a\Delta p$ and a uniform transmural pressure $\Delta p = p_{i0} - p_e$ we can write the governing differential equations as

$$\left.\begin{aligned}
&L_{11}(u)+L_{12}(v)+L_{13}(w)+(q_1+\nu q_2)\frac{\partial^2 u}{\partial\alpha^2}+q_2\left(\frac{\partial^2 u}{\partial\beta^2}-\frac{\partial w}{\partial\alpha}\right)-\mu_w\frac{\partial^2 u}{\partial t^2}=0\\
&L_{21}(u)+L_{22}(v)+L_{23}(w)+(q_1+\nu q_2)\frac{\partial^2 v}{\partial\alpha^2}+q_2\left(\frac{\partial^2 v}{\partial\beta^2}+\frac{\partial w}{\partial\beta}\right)-\mu_w\frac{\partial^2 v}{\partial t^2}=0\\
&L_{31}(u)+L_{32}(v)+L_{33}(w)-(q_1+\nu q_2)\frac{\partial^2 w}{\partial\alpha^2}-q_2\left(\frac{\partial u}{\partial\alpha}-\frac{\partial v}{\partial\beta}+\frac{\partial^2 w}{\partial\beta^2}\right)\\
&\qquad\qquad +(\mu_w+\mu_f)\frac{\partial^2 w}{\partial t^2}=0
\end{aligned}\right\} \tag{26}$$

The L_{ik}'s represent linear partial differential operators, μ_w and μ_f inertia quantities associated with the vessel wall and the fluid:

$$\mu_w = \frac{1-\nu^2}{Eh}a^2(\rho_w h) \tag{27}$$

$$\mu_f = \frac{1-\nu^2}{Eh}a^2 m_f \tag{28}$$

where m_f is the apparent or virtual mass of the fluid. According to Flügge [33] the linear differential operators are given by

$$
\left.\begin{aligned}
L_{11} &= \frac{\partial^2}{\partial\alpha^2}+\frac{1-\nu}{2}\frac{\partial^2}{\partial\beta^2}(1+c^2)\\
L_{22} &= \frac{\partial^2}{\partial\beta^2}+\frac{1-\nu}{2}\frac{\partial^2}{\partial\alpha^2}(1+3c^2)\\
L_{33} &= 1+c^2\left(\nabla^2\nabla^2+2\frac{\partial^2}{\partial\beta^2}+1\right)\\
L_{12} &= L_{21} = \frac{1+\nu}{2}\frac{\partial^2}{\partial\alpha\partial\beta}\\
L_{13} &= L_{31} = \nu\frac{\partial}{\partial\alpha}-c^2\left(\frac{\partial^3}{\partial\alpha^3}-\frac{1-\nu}{2}\frac{\partial^3}{\partial\alpha\partial\beta^2}\right)\\
L_{23} &= L_{32} = \frac{\partial}{\partial\beta}-c^2\frac{3-\nu}{2}\frac{\partial^3}{\partial\alpha^2\partial\beta}
\end{aligned}\right\} \tag{29}
$$

If we treat the shell as infinitely long, or assume that the boundary conditions are of appropriate form, the partial differential equations (26) can be satisfied by

$$
\left.\begin{aligned}
u &= A_{sk}\cos(ka\alpha)\cos(s\beta)\sin(\sigma t-\varepsilon)\\
v &= B_{sk}\sin(ka\alpha)\sin(s\beta)\sin(\sigma t-\varepsilon)\\
w &= C_{sk}\sin(ka\alpha)\cos(s\beta)\sin(\sigma t-\varepsilon)
\end{aligned}\right\} \tag{30}
$$

The substitution of (30) into (26) leads to a set of linear homogeneous equations for the coefficients A_{sk}, B_{sk}, C_{sk} containing σ as a free parameter. We require the existence of nontrivial solutions for A_{sk}, B_{sk}, C_{sk} and thus obtain as frequency equation relation (31).

Frequency equation:

$$
\begin{vmatrix}
-k^2a^2-\frac{1-\nu}{2}s^2(1+c^2) & \frac{1+\nu}{2}ka s & \nu ka+c^2\left(k^3a^3-\frac{1-\nu}{2}kas^2\right)\\
-(q_1+\nu q_2)k^2a^2-q_2s^2+\mu_w\sigma^2 & & -q_2ka\\
\frac{1+\nu}{2}kas & -s^2-\frac{1-\nu}{2}k^2a^2(1+3c^2) & -s-c^2\frac{3-\nu}{2}k^2a^2s\\
 & -(q_1+\nu q_2)k^2a^2-q_2s^2+\mu_w\sigma^2 & -q_2s\\
-\nu ka-c^2\left(k^3a^3-\frac{1-\nu}{2}kas^2\right) & \nu+c^2\frac{3-\nu}{2}k^2a^2s & 1+c^2[(k^2a^2+s^2)^2-2s^2+1]\\
+q_2ka & +q_2s & +(q_1+\nu q_2)k^2a^2+q_2s^2\\
 & & -(\mu_w+\mu_f)\sigma^2
\end{vmatrix} = 0 \tag{31}
$$

To determine the apparent mass m_f, we make use of the fact that the velocity potential corresponding to the perturbation w is of the form

$$
\phi_{sk} = -\frac{\sigma I_s(kr)}{kI_s'(ka)}C_{sk}\sin(ka\alpha)\cos(s\beta)\cos(\sigma t-\varepsilon) \tag{32}
$$

By definition, we have

$$-\rho_f\left(\frac{\partial\phi}{\partial t}\right)_{r=a} = m_f\frac{\partial^2 w}{\partial t^2} \tag{33}$$

From (33) we deduce

$$m_f = \rho_f\frac{I_s(ka)}{kI_s'(ka)} \tag{34}$$

We note that the determinant in (31) is a polynomial of third order in σ^2 with $s = 0, 1, 2, 3, \ldots$ and $k = 2\pi/\lambda$ as free parameters. For given initial stresses T_1^0 and T_2^0 we can determine from (31) the frequencies corresponding to each pair of values for s and k. As stability criteria we have again $\sigma^2(s, k) > 0$. If $\sigma^2 \leqslant 0$ for any kind of disturbances, the system is unstable.

Results of shell analysis

For the simulated arteries used in the experimental facility we find on the basis of equation (31) the stability boundaries ($\sigma^2 = 0$) and curves of constant amplification shown in Fig. 10. The curves are plots of the critical pressure difference as a function of the wave number ka for the parameter values corresponding to the laboratory model illustrated in Fig. 2:

$$\frac{h}{a} = 0{\cdot}1;\quad 0{\cdot}2$$

$$q_1 = 0{\cdot}15;\quad 0{\cdot}30$$

$$\sigma^2 = 0;\quad -4\times 10^4$$

We note that now, in contrast to the simplified membrane analysis, the minimum critical pressure difference for a given wave number corresponds to a unique value of s. The critical pressure difference is given in terms of mm Hg. The frequencies indicated on the abscissa correspond to a wave velocity (group velocity) of 650 cm/sec (see section 6). If we assume the duration of the instability to be 0·1 sec, the curve $\sigma^2 = -4\times 10^4$ represents the pressure differences necessary to produce amplifications of the order $\exp|\sigma|\tau = \exp 20$ for disturbances with the appropriate spatial variation defined by s and k. From the fact that in each case the curves $\sigma^2 = 0$ and $\sigma^2 = -4\times 10^4$ almost coincide, we conclude that the system is highly unstable and thus acts as a strong amplifier as soon as $p_e > p_{io} - (\Delta p)_{crit}$. The rapid increase (note the logarithmic scale) of the critical pressure difference with the wave number ka predicts the clinical and laboratory observations that the Korotkoff sounds near the diastolic pressure have predominantly low frequency components and that with increasing cuff pressure the sounds not only become more intense but also begin to include components with a higher pitch. Besides this, from Fig. 10 and the frequency equation (31) we conclude that the results of the stability analysis based on the shell model confirm the findings of the membrane analysis regarding the effects of the cuff length, h/a, E, $T_{1\,0}$ and $\rho_w h$ on the diastolic auscultatory pressure. We also note that $(-\Delta p)_{crit} = 6$ mm Hg for the simulated artery ($h/a = 0{\cdot}1$, $a = 1{\cdot}59$ cm, $q_1 = 0{\cdot}15$, $E = 6{\cdot}9\times 10^6$ dyn/cm^2, $\nu = 0{\cdot}5$). Even though this pressure difference $(-\Delta p)_{crit}$ is smaller than the values observed experimentally for diastole [18], it can be considered a good approximation since the cuff pressure readings for the cessation of the Korotkoff

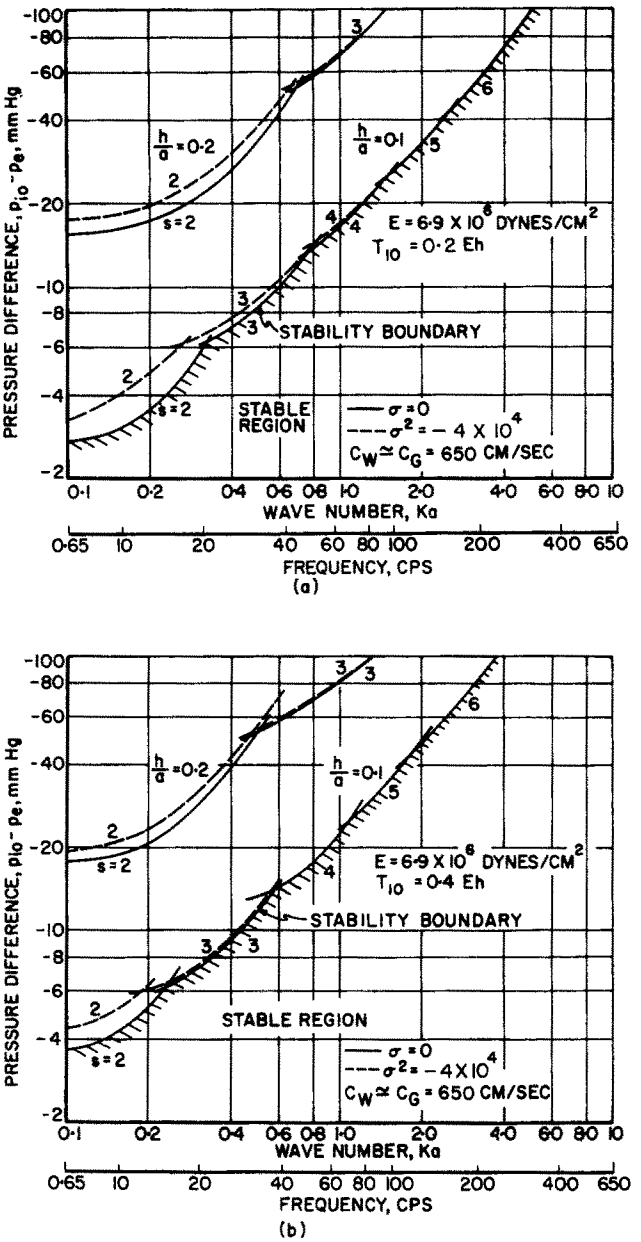

FIG. 10 Stability boundaries and amplification curves for the shell model.

sounds are in general higher than the optimal value because of the imperfect auditory acuity of the observer. In the experiment the cuff pressure was reduced at a rate of approximately 3 mm Hg/sec as in clinical practice, and since the Korotkoff sounds occur at the pulse rate we can expect an error of up to 3 mm Hg.

6. AMPLIFICATION OF MOVING DISTURBANCES

For the sake of simplicity we have so far ignored the inertia effects associated with the propagation of disturbances in our stability analysis described in the preceding section. Taking the compressibility of the fluid into consideration we can write the expressions for the velocity potential and the radial wall displacement corresponding to a propagating disturbance in the form

$$\Phi(x, \beta, r, t) = \gamma I_s\left(\zeta \frac{r}{a}\right) \exp[i(kx + s\beta - \omega t)] \tag{35}$$

$$w(x, \beta, t) = \frac{\zeta}{ia\omega} \frac{I_s'(\zeta)}{I_s(\zeta)} \Phi(x, \beta, a, t) \tag{36}$$

where

$$\zeta = \sqrt{\left(k^2 a^2 - \frac{\omega^2 a^2}{C_f^2}\right)} \tag{37}$$

$$ka = k_1 a - ik_2 a \tag{38}$$

and where ω is the circular frequency of the moving disturbance with the wave number k and C_f the speed of sound of the fluid. The velocity potential defined by (35) satisfies the continuity equation

$$\frac{1}{C_f^2} \frac{\partial^2 \Phi}{\partial t^2} = \nabla^2 \Phi \tag{39}$$

The radial displacement (36) complies with the kinematic boundary condition (4):

$$\left(\frac{\partial \Phi}{\partial r}\right)_{r=a} = -\frac{\partial w}{\partial t}$$

Restricting ourselves to the membrane model we require Φ and ω to satisfy the dynamic boundary condition (15) and obtain as frequency equation

$$a^2\omega^2\left[\rho_w h + \rho_f a \frac{I_s(\zeta)}{\zeta I_s'(\zeta)}\right] = \frac{Eh}{1-\nu^2} + a\Delta p(s^2 - 1) + k^2 a^2 (T_{10} + va\Delta p) \tag{40}$$

in which ζ and ka are complex numbers. We notice that equation (40) reduces to the "old" frequency equation (18) if we take $k_2 = 0$, $C_f = \infty$ and define $\omega^2 = \sigma^2$. While equation (18) yielded as criterion for instability $\sigma^2 < 0$ we now have to require for instability

$$k_2 > 0 \quad \text{for real } \omega \tag{41}$$

Since the expression

$$\chi = \rho_f a \frac{I_s(\zeta)}{\zeta I_s'(\zeta)} = \chi_R + i\chi_I \tag{42}$$

can have a negative real part with a magnitude $|\chi_R| > \rho_w h$ with $k_2 > 0$ we have essentially established the approximate equivalence of the stability criteria (41) and $\sigma^2 \leqslant 0$ and the fact that certain moving disturbances are also greatly amplified. Equation (40) yields

k_1 and k_2 as functions of ω for given physical and geometric parameters. As phase velocity of a disturbance moving through the unstable section of the artery we have

$$C_w = \frac{\omega}{k_1} = \frac{2\pi f}{k_1} \tag{43}$$

For a first appraisal of our analysis and results we forego the extensive numerical work

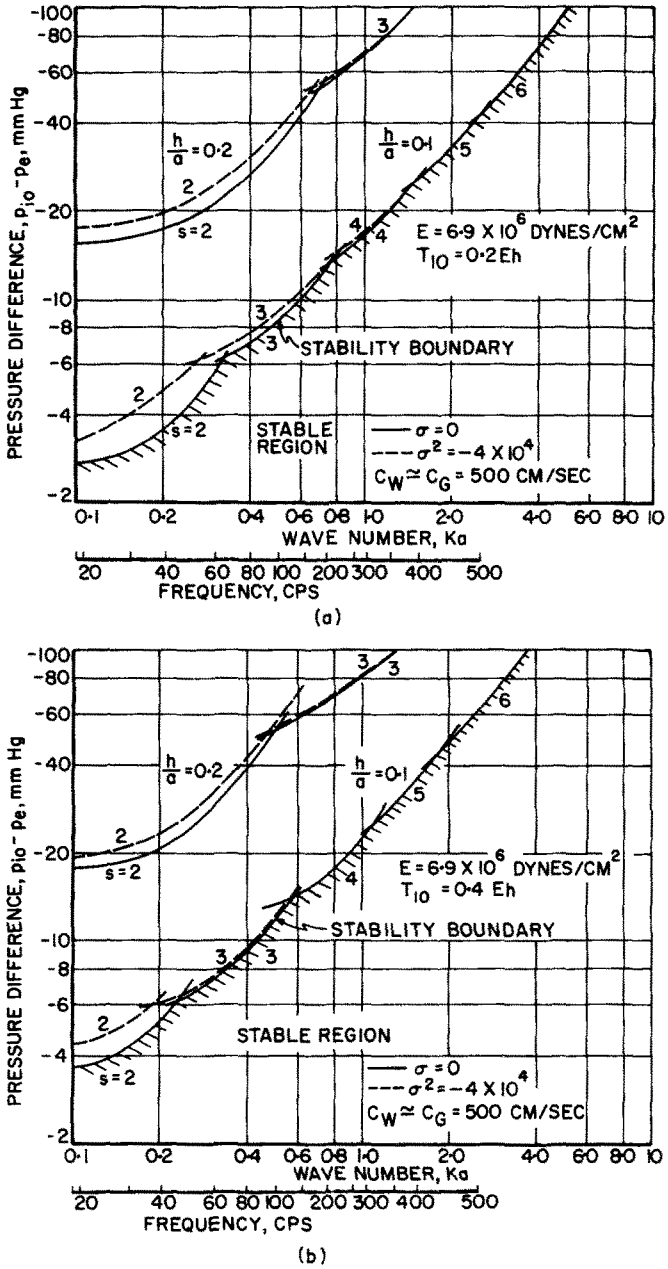

FIG. 11. Stability boundaries and amplification curves for a human brachial artery based on estimates of the physical and geometric parameters for *in vivo* conditions.

required to obtain the solutions $k_1(\omega)$, $k_2(\omega)$ from equation (40) and assume that the disturbances considered in section 5 move with the experimentally determined group velocity C_G (see Fig. 5) through the unstable segment of the tube. In other words, we assume the vibration frequency f (cps) to be related to the wave length λ of the disturbance by

$$\lambda . f = C_G \tag{44}$$

For our laboratory model we have taken as representative group velocity for the diastolic phase

$$C_G = 650 \text{ cm/sec}$$

The corresponding frequency scale is indicated in Fig. 10.

7. NUMERICAL RESULTS OF THE STABILITY ANALYSIS OF THE HUMAN BRACHIAL

For a quantitative investigation of the stability of the human brachial artery during the application of the sphygmomanometer it is necessary to know the pertinent geometric and physical parameters of the brachial *in vivo*. Unfortunately we lack *in vivo* data on the parameters defining the elastic properties and the tonus. Limited measurements have been made on four human brachials obtained at autopsy; all of which were initially pressurized to 300 mm Hg and deflated to zero several times in order to eliminate hysteresis and thus assure repeatable results for the pressure–displacement data [34]. It appears from these measurements that the values of the parameters $h/a = 0{\cdot}1$, $0{\cdot}2$, $E = 6{\cdot}9 \times 10^6$ dyn/cm^2, $\nu = 0{\cdot}5$, $T_{10}/Eh = 0{\cdot}2$, $0{\cdot}4$, $\rho_w = 1{\cdot}06$ g/cm^3 and $\rho_f = 1{\cdot}00$ g/cm^3 selected for the experimental model represent reasonable order-of-magnitude estimates for the human brachial. We therefore can make use of the results obtained in section 5.2 for the simulated brachial but have to account for the smaller radius of the brachial ($a \approx 0{\cdot}4$ cm instead of $a = 1{\cdot}59$ cm). This change in radius merely causes a change in the frequency scale shown in Fig. 10 by a factor 3·06 if we assume that the wave velocity of the brachial artery during the diastolic phase is approximately 500 cm/sec. For the human brachial we thus find the stability boundaries ($\sigma^2 = 0$) and curves of constant amplification ($\sigma^2 = -4 \times 10^4$) given in Fig. 11.

We note that the conclusions deduced in section 5 from the theoretical analysis equally apply for the human brachial. Furthermore, we see from Fig. 10 that for the assumed parameter values the range of $(-\Delta p)_{crit}$ is approximately $+2{\cdot}7$ to $+15{\cdot}5$ mm Hg for h/a values between 0·1 and 0·2. (These values for $(-\Delta p)_{crit}$ increase, of course, proportionately if Young's modulus is increased.) This result compares favorably with the clinical data cited in [3] according to which the auscultatory error can be as much as 25 per cent of the intraluminal pressure.

8. CONCLUSIONS AND DISCUSSION

The theoretical and experimental results of this investigation support the hypothesis that the Korotkoff sounds at diastole are due to a dynamic instability of the brachial artery, the instability being induced by the application of a pressure cuff. However, for further substantiation the experimental studies conducted so far should be extended to

include recordings of the actual dynamic response of the compressed portion of the blood vessel or its simulated counterpart during the generation of Korotkoff sounds. We can readily incorporate the effects of the semi-fluid tissue surrounding the brachial artery in a mathematical formulation. An extension of the theory to include

(a) effects of a nonisotropic elastic behavior of the blood vessel,
(b) the time variation of the pulse pressure during the Korotkoff sound generation,
(c) the nonuniformity of the pressure exerted by the cuff on the brachial,
(d) the viscosity of the blood and surrounding medium, and
(e) nonlinear effects of large displacements and velocities

would entail a substantial increase of the complexity of the analysis. But for an accurate theoretical prediction of the Korotkoff sound spectrum, some of the effects listed above may have to be taken into account. Beside this, the availability of reliable data on the elastic properties of the brachial *in vivo* would be required.

Acknowledgements—The authors are indebted to Eric Ogden, M. D. and Gertrud Anliker, M. D. for their interest and medical counsel and to Dr. I-Dee Chang for stimulating discussions. They also wish to thank Dr. W Flügge for his helpful comments on the shell analysis and Mr. J. Crumal for his assistance in conducting the experiments.

REFERENCES

[1] C. R. Smith and W. H. Bickley, *The Measurement of Blood Pressure in the Human Body*. (Technology Survey). NASA SA-5006 (April 1964).
[2] W. F. Ganong, *Review of medical Physiology*. Lange Medical Publications (1963).
[3] G. W. Pickering, *High Blood Pressure*. Grune and Stratton (1955).
[4] N. S. Korotkoff, A Contribution to the problem of methods for the determination of the blood pressure. *Rep. imp. Med. Acad., St. Petersburg* **II**, 365 (1905).
[5] J. A. MacWilliam and S. Melvin, The estimation of diastolic pressure in man and *in Vitro*. *Heart* **5**, 153 (1913–14).
[6] Joseph Erlanger, Studies in blood pressure estimation by indirect methods. Part II—The mechanism of the compression sounds of Korotkoff. *Am. J. Physiol.* **40**, 82 (1916).
[7] M. J. Erskine, *Blood Pressure Sounds and Their Meanings*. Springfield (1957).
[8] L. P. Pressman, A contribution to the estimation of the results of measurements of blood pressure taken, by Korotkoff's sound method. *Med. Times, N.Y.* 419 (Oct. 1936).
[9] R. L. Lange, R. P. Carlisle and H. H. Hecht, Observations on vascular sounds: "The pistol-shot" sound and the Korotkoff sound. *Circulation* **8**, 873 (June 1956).
[10] R. L. Lange and H. H. Hecht, Genesis of pistol-shot and Korotkoff sounds. *Circulation* **13**, 975 (Nov. 1958).
[11] D. Chungcharoen, Genesis of Korotkoff sounds. *Am. J. Physiol.* 190 (July 1964).
[12] C. Bramwell, Blood-pressure and its estimation. *Lancet*, pp. 138–140 and pp. 184–188 (Jan. 1940).
[13] V A. McKusick, Symposium on cardiovascular sound (I). Mechanisms. *Circulation* **16**, 270 (1957).
[14] D. H. Hooker and J. D. Southworth, Interpretation of the auscultatory blood pressure sounds. *Archs intern. Med.* **13**, 384 (1914).
[15] H. M. Korns, The nature and time relations of the compression sounds of Korotkoff in man. *Am. J. Physiol.* **76**, 247 (1926).
[16] F. Groedel and M. Miller, Graphic study of auscultatory blood pressure measurement. *Expl Med. Surg.* **1**, 148 (1943).
[17] M. B Rappaport and A. A. Luisada, Indirect sphygmomanometry. *J. Lab. clin. Med.* **29**, 638 (1944).
[18] A H. Sacks, K R. Raman and J A. Burnell, A study of auscultatory blood pressure in simulated arteries. Part 4, *Proc 4th Int Congr. on Rheology*, edited by A. L. Copley, pp 215–230. Interscience (1965).
[19] E. A. Fox and Edward Saibel, Attempts in the mathematical analysis of blood flow. *Trans. Soc Rheol.* 7, 25 (1963).
[20] K. R. Raman, Experimental study of the mechanical behavior of a flexible fluid-filled tube simulating arteries. Engineer's Thesis, Department of Aeronautics and Astronautics, Stanford University (1964).
[21] D. A. McDonald, *Blood Flow in Arteries*. Williams and Wilkins (1960).

[22] HANS ZIEGLER, On the concept of elastic stability. *Adv. appl. Mech.* **4**, 351 (1956)
[23] M. A. BIOT, *Mechanics of Incremental Deformations*. Wiley (1965).
[24] V. V. BOLOTIN, *Dynamic Stability of Elastic Systems*. Holden Day (1964).
[25] A. E. ARMENAKAS and G. HERRMANN, Vibrations of infinitely long cylindrical shells under initial stress *AIAA Jnl* **1**, 100 (1963).
[26] ERIC MOLLO-CHRISTENSEN, Energy exchange and stability considerations in the circulatory system. MIT Fluid Dynamics Research Laboratory Report No. 61–7 (1961).
[27] ERIC MOLLO-CHRISTENSEN, Wave propagation, dispersion, and energy transport in arterial blood flow. To be published in the *Proc. 11th Int. Congr. Appl. Mech.* Munich, 1964.
[28] J. W. LAMBERT, On the nonlinearities of flow in nonrigid tubes. *J. Franklin Inst.* **266**, 83 (1958).
[29] M. N. L. NARASIMHAN, Mechanics of flow of real fluids through flexible tubes. *J. Sci. Engng Res. Indian Inst. Tech. Kharagpur* **4**, 91 (1960).
[30] E. H. BLOCK, A quantitative study of the hemodynamics in the living microvascular system. *Am. J. Anat.* **110**, 125 (1962).
[31] D. A. MCDONALD and E. P. W. HELPS, Streamline flow in veins. Welcome Film Unit (1954).
[32] M. J. KARVONEN, L. J. TELIVUO and E. J. K. JÄRVINEN, Sphygmomanometer cuff-size and the accuracy of indirect measurement of blood pressure. *Am. J. Cardiol.* 688 (May 1964).
[33] W. FLÜGGE, *Stresses in Shells*. Springer (1960).
[34] E. G. TICKNER and A. H. SACKS, Theoretical and experimental study of the elastic behavior of the human brachial and other human and canine arteries. Vidya Rep. No. 162 (Nov. 1964).

(*Received* 2 *October* 1965)

Résumé—Une analyse théorique du phénomène des sons Korotkoff à la diastole est présentée avec des résultats expérimentaux. La formulation de l'analyse mathématique est basée sur des faits dérivés d'expériments fondamentales avec un modèle de laboratoire qui simule l'artère brachiale et le sphygmomanomètre et qui démontrent les sons Korotkoff sous conditions contrôlées. Les sons Korotkoff à la diastole sont interprétés comme un phénomène d'instabilité dynamique, oscillations d'une amplitude allant s'aggrandissant, l'instabilité étant induite par l'application d'un manchon faisant pression. Les résultats de l'analyse vérifient les observations expérimentales en ce qui concerne la longueur du manchon, l'épaisseur et l'élasticité du vaisseau à la pression diastolique. Ils produisent également de bonnes approximations pour la différence entre la pression auscultatoire diastolique et le minimum véritable de la pression dans l'artère simulée aussi bien que dans la brachiale humaine. Le résultat indique que le résultat auscultatoire est toujours plus élevé que le minimum véritable de la pression dans le vaisseau par un degré qui dépend des propriétés physique et géométriques du vaisseau. A part cela, l'analyse théorique prédit que les sons Korotkoff près de la pression diastolique ont des composants à basse fréquence prédominante et avec la pression du manchon augmentant, les sons non seulement deviennent plus intenses mais aussi commencent à inclure des composants ayant une plus grande hauteur de son.

Zusammenfassung—Es wird eine theoretische und experimentelle Analyse der Erscheinung von Korotkoff Tönen bei der indirekten Bestimmung des Blutdruckes präsentiert. Die mathematische Formulierung der Theorie beruht auf grundlegenden Versuchen an einem Laboratoriumsmodell welches die arteria brachialis und die Manchette des Blutdruck Apparates nachahmt und Korotkoff Töne unter kontrollierten Bedingungen erzeugt. Die Korotkoff Töne während der diastolischen Phase der Blutdruckmessung sind als eine Erscheinung von dynamischer Unstabilität (Schwingungen mit exponentiell wachsenden Amplituden) dargestellt wobei die Unstabilität durch die Druckmanchette verursacht wird. Die analytische Ergebnisse bestätigen Versuchsbeobachtungen hinsichtlich der Einflüsse der Manchettenlänge, der Wanddicke und Elastizität der Arterie auf den Messwert des diastolischen Druckes. Ausserdem geben sie gute Annäherungen für den Unterschied zwischen dem auskultierten diastolischen Druck und dem wahren Mindestwert des Druckes in der simulierten Arterie sowie in der brachialis. Die Ergebnisse zeigen, dass der auskultierte Messwert immer höher ist als der wahre Mindestwert des intraluminalen Druckes. Der Unterschied hängt von den physikalischen und geometrischen Eigenschaften des Gefässes ab. Die theoretische Analyse indiziert ausserdem, dass die Korotkoff Töne in der diastolischen Phase der Blutdruckmessung überwiegend niedrige Frequenzkomponenten aufweisen und dass mit zunehmendem Manchettendruck die Töne nicht nur stärker werden aber auch beginnen höhere Frequenzkomponenten einzuschliessen.

Абстракт—Предлагается на рассмотрение теоретический анализ явления звуков Короткова при диастоле, вместе с экспериментальными результатами. Формулировка математического анализа основывается на фактах, полученных из основных опытов с лабораторной моделью, которая симулирует плечевую артерию и сфигмоманометр и, которая образует звуки Короткова при конт-

ролируемых условиях. Звуки Короткова при диастоле объясняются, как явление динамической неустойчивости (колебания с увеличенной амплитудой), неустойчивости, которая вызывается применением манжеты давления. Результаты анализа подтверждают экспериментальные наблюдения относительно эффектов длины манжеты, толщины стенки и эластичности сосуда под диастолическим давлением. Они также хорошо согласуются с разницей между диастолическим давлением, полученным путём выслушивания и действительным минимумом давления в симулируемой артерии, так же, как и в человеческой плечевой артерии. Результаты указывают на то, что показания путём выслушивания всегда выше, чем действительный минимум давления, находящегося в просвете на количество, которое зависит от физических и геометрических свойств сосуда. Кроме того, теоретический анализ предсказывает, что звуки Короткова вблизи диастолического давления обладают компонентами преимущественно низкой частоты и, что с увеличением давления манжеты, звуки не только становятся более интенсивными, но также начинают включать компоненты с большей высотой звука.